Gas Permeation Models for Dilatant Deformation of Rock Salt under Deviatoric Stress Conditions

Guenter Pusch[1]

Plyn permeačné modely pre dilatačnú deformáciu kamennej soli pri podmienkach deviatorického napätia

Permeability of 30 rock salt cores were measured under various deviatoric stress conditions. A triaxial cell was designed and built to measure the hydraulic properties such as the pore volume and permeability during the compression experiments. To determine variations in the pore volume, a high precision pump was used and the pore volume changes as well as the gas permeabilities were recorded continuously as a function of time and stresses. A permeability reduction in the compression stage is not obvious although the decrease of pore volume appears to be a controlling phenomenon of the compression. Similarly to previous studies, a spontaneous increase in the permeability was observed shortly after the dilatancy boundary was exceeded, separating the compression from the dilatant deformation phase. At the end of the dilatant deformation, the permeability reaches a plateau value which afterward remains approximately a constant for low stress rates up to the fracture pressure. This allows the percolation of gas along the extended grain boundaries of the salt crystals and through the inter-crystalline flow paths and yields an increase of the permeability of 3 to 6 tens of order. Combined acoustic emission measurements performed with 8 sensors showed that the percolation begins equally throughout the core at the same time. The dilatancy and permeability are found to be controlled by many factors,most importantly by the minimal principal stresses. The end porosities of the stressed cores were correlated with the permeability in the form of a Kozeny-Carman type relationship. Semi-empirical and percolation flow models were applied to match the observed flow characteristics of cores with corresponding properties of the excavation damaged zone in the Asse salt mine.

Key words: ***Dilatant Deformation of Rock Salt,*** *permeability, flow models*

Introduction

The rock salt is considered to behave as an ideal caprock under reasonably high confining pressures. Its tightness is related to the crystal structure and the visco-plastique deformability under high pressure conditions. However this ideal characteristics is only valid if the integrity of the rock salt is not disturbed by tectonic movements or artificial excavations like caverns or shafts involved in underground repositories. The excavation damaged zone (EDZ) along walls of underground cavities is a potential pathway for a waste migration. Modelling of the fluid transport along the EDZ has been a target of many experimental and in-situ studies.

Interpretations from in-situ gas permeability tests have shown that the EDZ has only a limited extension into the intact rock salt formation.

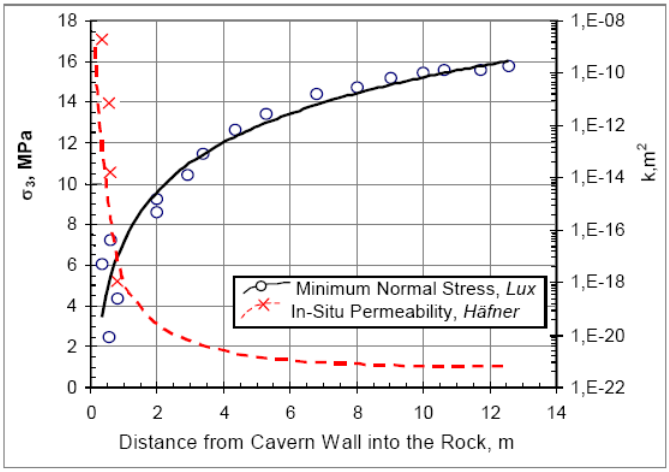

Fig. 1. Simulated and measured permeabilities in the EDZ of an underground salt mine

Nomenclature:

A correlation coefficient

B correlation coefficient

C power law-factor in the Kozeny-Carman equation

c mean crack radius, L

c_p pore volume compressibility, $M^{-1}LT^2$

k permeability, L^2

k_1 permeability at the axial stress σ_1, L^2

k_3 permeability at the hydrostatic stress $\sigma_1 = \sigma_3$, L^2

[1] *Guenter Pusch*, TU Clausthal, H. Alkan, GRS-ISTec, Abt. Analyse, Köln, Germany
(Recenzovaná a revidovaná verzia dodaná 8. 1. 2007)

l crack spacing, L
m dilatancy exponent
n compression exponent
P* percolation probability
t critical percolation exponent
α crack shape factor/ and the iot-coefficient
θ hydraulic aperture shape and drag factor
ε_v volume dilatancy
φ porosity
ω crack width, L
σ normal stress, $ML^{-1}T^{-2}$
σ_1 axial stress, $ML^{-1}T^{-2}$
σ_3 radial stress, $ML^{-1}T^{-2}$
σ_f shear-stress failure boundary, $ML^{-1}T^{-2}$
ν Poisson constant

The simulated data of the permeability extension with the distance from the cavern wall were determined with a mechanical model, calculating the dilatant pore-volume related permeability increase, caused by a difference between the radial and the tangential stress across the surface of the wall. The focal point of the coupling of mechanical and hydraulic properties of salt was the progressive experimental and modelling work of Stormont, Serrata and Fuenkajorn in the early 90ies, who have applied the model theory of capillary networks of sedimentary rocks for the correlation of porosity and permeability of salt as it was learned from Kozeny and Carman. The φ-k-correlation as a coupling algorithm seemed to be useful because the porosity change by dilatant effects is a geometrical factor, which can be integrated into the stress - strain relationship of mechanical models. The decisive difference between the rock salt and sedimentary rocks is the reasonably large primary porosity of sedimentary rocks, compared to the nil porosity of the intact rock salt. Consequently, without a change in the porosity, the permeability of the damaged zone could increase by a magnitude of several decades. Peach and Spears have concluded that the exponential increase of the salt rock permeability under deviatoric stress conditions must be caused by the opening of existing inter-crystalline boundaries or by the creation of intra-crystalline micro-fractures. The permeability development can therefore not be modelled by simple geometrical algorithms based on the crack width

$$k = \frac{4\pi\omega^3 c^2}{15l^3} \tag{1}$$

The application of the geometry based micro-fracture network model as for example the Warren-Root-Model, the Chen and the Bai- Cubic Law Model as well as the Dual Porosity Models from Kazemy, Chen and Teufel, which were successful in modelling fracture networks in sedi-mentary rocks, failed in the interpretation of permeability dilatancy effects of rock salts.

The statistics was introduced in the development of fracture networks based on fractal dimensions of penny-shaped cracks in the percolation theories published by Halperin, Feng, Sen, Guegen und von Dienen as well as by Peach.

$$k = \frac{2\omega^2 \alpha\theta\varepsilon_v P^*}{15} \tag{2}$$

The development of the number of micro-cracks is correlated with a threshold value of interconnected cracks, which can form a continuous flow path for the migrating fluid. This physical theory provides a good basis for modelling the exponential increase of permeability in the EDZ after exceeding a critical deviatoric stress resulting in a dilatant deformation of rock salt. Besides the physical correlations, empirical correlations exist, which are nothing more than a mathematical fit of the experimental permeability performance. Such empirical correlations have been published by Pusch and Weber for a dilatant deformation of crystalline rocks with the following formula.

$$\frac{k_1}{k_3} = \left(\frac{\sigma_1}{\sigma_3}\right)^{-n} \exp\left[A\left(\left(\frac{\sigma_1}{\sigma_3}\right)^{m} - 1\right)\right] \tag{3}$$

The first term represents the compression effect of the hydrostatic deformation and the second term the dilatancy effect, which are superposed in the equation. The coefficient A determines the minimum of the function or the dilatancy boundary (begin of inelastic disintegration) and can therefore be equalled with the maximal elastic lateral strain in the biaxial Hook`s Law. This yields:

$$\frac{k_1}{k_3} = \left(\frac{\sigma_1}{\sigma_3}\right)^{-n} \exp\left[\frac{n}{m}\left(\frac{\nu}{1-\nu}\right)\left(\left(\frac{\sigma_1}{\sigma_3}\right)^{m} - 1\right)\right] \tag{4}$$

In this experimental study rock salt samples from the Asse salt mine have been investigated to study the development of the dilatant process, which causes the rock damage. Based on this measurements, a correlation function had to be developed, which could be used as an integral element for the coupling of the mechanical and hydraulic model.

Experimental

Core samples from the Asse Salt Mine in Germany were collected in intact rock salt area with a cylindrical shape, the diameter of 6 cm and a the length of 30 cm. The compact samples were mounted in the pressure cell of a triaxial-permeameter.

Tab. 1. Technical Data of Triax-Permeameter Cells.

Maximal Core Diameter and Length, [mm]	**T 100**	**T 300**
	30/100	60/300
Max. Axial Stress, [Mpa]	230	80
Max. Radial Stress, [Mpa]	160	50
Volume Change Accuracy, [µl]	-	10
Permeability Resolution,[m^2]	10^{-20}	10^{-20}
Max. Temperature, [°C]	90	60

Two different cells for various ranges of operating conditions are included in the rig, their features are summarized in Table 1. The axial and radial stress on the core sample are controlled by a hydraulic unit and an electronic control device, which allow an independent rate control on the axial and the radial load. The experimental design of the compression or extension test is programmable via the Diadem PC-software. The sample deformation was controlled by measuring the volume dilatancy of the cylindrical sample through a precise micro-liter pump and a strain gauge for the axial deformation. In the end faces of the cylindrical core sample and in the outer walls of the rock salt, acoustic sensors / converters from lead, zirconium and titanat are placed in 3 equidistant planes along the axis and shifted at an angle of 120 °. The acoustic emissions can thereby be measured and registered in the PC-measurement system, using an 8-channel transient recorder chip.

The end plates from Teflon were used in order to reduce the high friction between the steel pistons and the end faces of the core sample. An excessive friction may hinder the equal extension of the end-zone of the core sample resulting in an intensive compaction of end-zones. As a consequence, the permeability changes will not be equally distributed along the axis of the core. Most core samples are characterized by an artificial permeability due to the release of stresses after coring. This artificial permeability has to be compensated by a re-compaction of the core sample before the measurement begins. The re-compaction was achieved by an iso-static loading of 5 MPa for several hours. The gas flow through the cell and the core sample is controlled by a gas pressure regulator at a constant entrance pressure between 1 and 3 MPa and a mass flow detector or, in the case of liquid flow, by a precise piston pump at the inlet and outlet of the cell. This assembly allows the application of back-pressure during the test.

In this study 30 tests have been performed under various conditions of the initial radial stress, loading rates of axial stress, pressure gradients for the gas flow, pore pressure, and the morphology of grains in the rock salt. The results of this study are presented in the paper "Definition of the Dilatancy Boundary Based on Hydro-Mechanical Experiments and Acoustic Detection", SMRI2002.

In Figure 2, the measured properties of a compression test on an Asse rock salt sample, typical for this study, is shown. The initial radial stress after the re-compaction of the sample was 3 MPa and it was kept constant during the test.

The permeability for gas can be calculated from the recorded mass flow values at the constant pressure gradient of 5 MPa/m using the corrected Darcy-formula for compressible media. For this primarily phenomenological experiments, the Klinkenberg-correction of the absolute permeabilities was not considered.

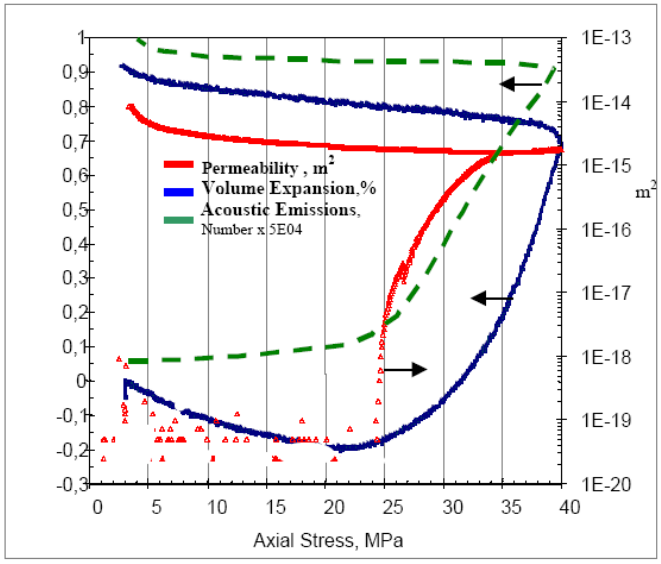

Figure 2 shows the volume change of the rock sample measured by the micro-liter pump, which yields a negative value during the compression phase of the experiment until a minimum is reached. The parallel observation of the gas flow is marked by a rather high scattering of data, due to the changing flow paths in an irregular network of inter-crystalline porosities of the re-compacted sample.

Fig. 2. Typical compression test of poro-perm dilatancy on the Asse Rock Salt
Sample AT3-011, σ_3 = 3 MPa, the axial stress loading rate = 0,4 MPa/min

However, when the compression–dilatancy boundary (C/D boundary corresponding to the minimum in the volume expansion curve) is reached, the acoustic emission, the permeability and the volume expansion begin to increase sharply and steadily. The dilatant deformation ends when the permeability curve begins to level off which is indicative for a sustainable plastic deformation. The build-up phase of the test was then terminated in order to avoid the fracture of the sample. The draw-dawn phase of the test is accompanied by a levelling of the gas permeability and a rather small increase of the volume expansion corresponding to minor acoustic emissions.

The volume change of the sample, measured with the micro-liter pump was used to the calculate porosity changes based on the assumption that the salt matrix is in-compressible. After terminating of the test the sample was dismounted from the cell and the actual porosity was measured by the brine saturation method. The end-values were used to calibrate the porosity changes during the compression test. The recorded acoustic emissions were introduced into the percolation model for calculating of the permeability.

Figure 3 represents a correlation of the end-values of porosities and the gas permeabilities of the EDZ. A correlation formula is given which is based on the classical Kozeny-Carman approach.

$$k = 3(\phi)^{2,29} \tag{5}$$

(k is expressed in Milli-Darcies if φ is introduced in percentage)

$$k = k_0 \frac{\exp(-Cc_p\Delta\sigma)}{1-\phi_0\exp(-c_p\Delta\sigma)} \tag{6}$$

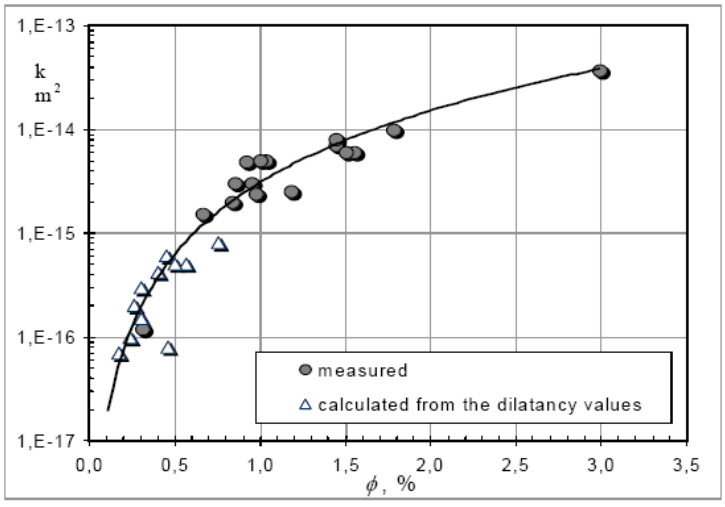

Fig. 3. Correlation of poro-perm dilatancies for the EDZ in the Asse Rock Salt .

Hydraulic Modelling of the Gas Permeation under Dilatant Deformation Conditions

Two conceptual structure models of rock salt can be considered as a starting point for the permeability development:

1. **The Structurally Dense Salt Model**

This model is based on a infinitely small primary porosity and humidity of the salt. The crystals are in a perfect dense arrangement without voids along grain boundaries.

2. **The Fluid Residue Model**

This model is based on the assumption that traces of the residual brine can be found along certain grain or crystal boundaries resulting in a primary porosity.

The hydraulic models based on these structural models, will be called the "**Dilatant Permeability Model**" and the "**Displacement Flow Model**".

The dilatant permeability model is a one-phase-flow model, which can be derived from the percolation theory of the generation and the propagation of inter-crystalline or trans-crystalline voids, interfering into a network of flow paths, caused by the deviatoric stress situation in the rock specimen. For the displacement flow model, one or two phase-flow-concepts can be applied based on the capillary threshold pressure concept of the displacement of wetting fluids by non-wetting.

In this paper the structurally dense model is favoured and therefore the dilatant permeability model is used.

Semi-empirical Hydraulic Models for the Dilatant Permeability Concept

The correlation formulas of geometric changes and stress conditions for example the **Hou** and **Lux** Model, taking into account anisotropic and time dependent effects (creeping) of the mechanical deformation, include many parameters of a tensor character (stress and strain), which are physically correct but very difficult to measure in experiments. Therefore, empirical correlations have been often used to couple directly the permeability change and the stress deviator (σ_1 - σ_3).

An example of such a correlation for crystalline rocks is given in the following Figure 4 with the formula correlated by Pusch/Weber which includes the shear stress failure boundary σ_f and is applicable for the poro-elastic deformation.

$$\frac{k_1}{k_3} = \left(\frac{\sigma_1}{\sigma_3}\right)^{-n} \exp\left[A\left(\frac{\frac{\sigma_1}{\sigma_3}-1}{\frac{\sigma_f}{\sigma_3}-\frac{\sigma_1}{\sigma_3}}\right)^{m}\right] \tag{7}$$

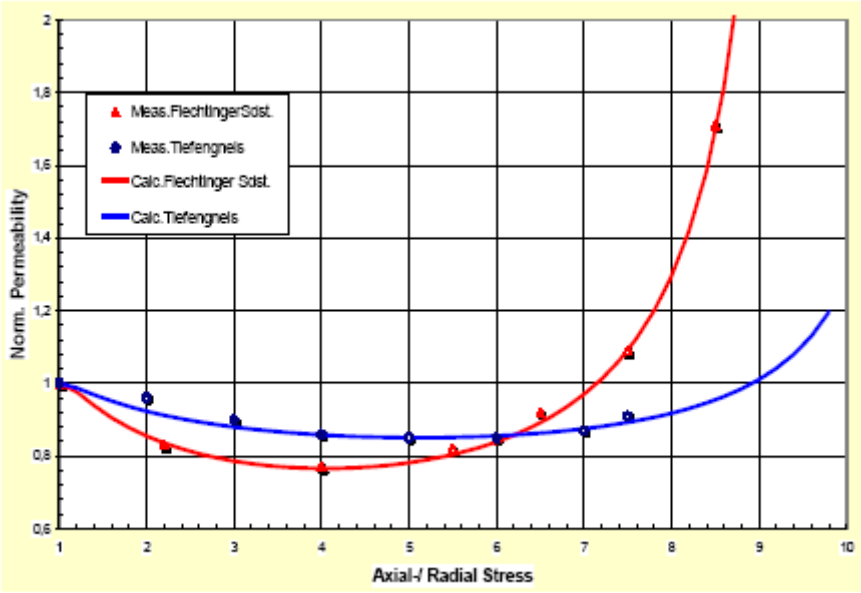

Fig. 4. Permeability-dilatancy experiments with Rotliegendes sandstones and crystalline Rocks matched by the semi-empirical poro-elastic correlation by Pusch/Weber.

For the poro-plastic deformation of salt specimens, a completely different permeability performance was observed in experiments presented in this study, which could be fitted by the following formula after Alkan and Cinar:

$$\frac{k_1}{k_3} = \frac{1}{2}\left[\left(\frac{\sigma_1}{\sigma_3}\right)^{-n} + A^{1-\exp\left(-cB^m\right)}\right] \tag{8}$$

$$A = \frac{1}{2}\left[6\cdot 10^5 \exp\left(-0{,}89\sigma_{3eff}\right)\right] \qquad \sigma_{3eff} = \sigma_3 - \alpha p \qquad B = \left(\frac{\sigma_1}{\sigma_3} - \frac{\sigma_{1C/D}}{2}\right)$$

Dilatancy Boundary

This empirical model was adopted to the experimental conditions in order to define the fitting parameters. It could be successfully applied to match the compression experiments with the Asse rock salt, as it can be seen from Fig. 5 and 6.

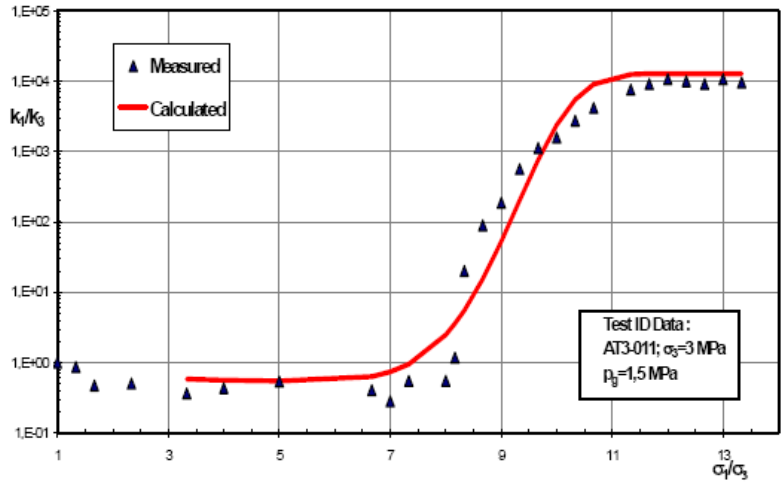

Fig. 5. Permeability-dilatancy experiment for Asse rock salt matched by the poro - plastic correlation after Alkan/Cinar .

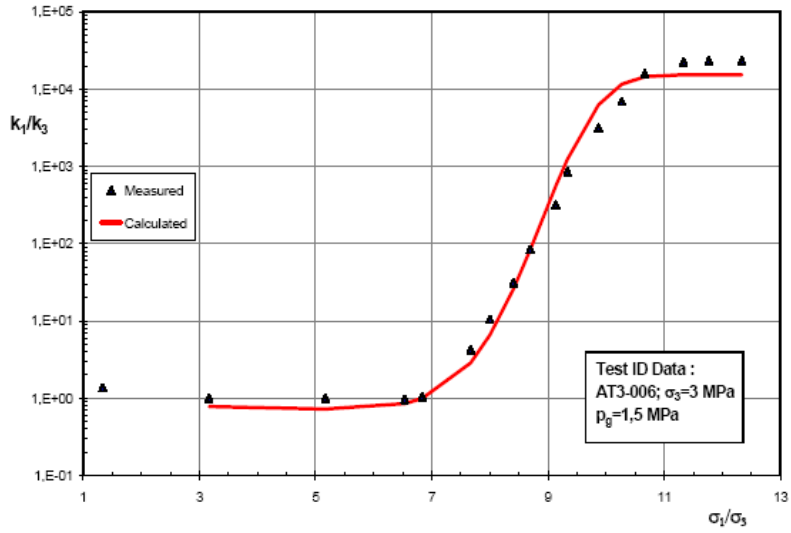

Fig. 6. Permeability-dilatancy experiment for Asse rock salt matched by the poro- plastic correlation after Alkan/Cinar

The fitting parameters for the 2 experiments presented in the previous figures are given in Table 2.

Test ID No	σ_3 MPa	$\sigma_{1C/D}$ MPa	p_g MPa	A_4 $10^{}$	B	c 10^{-6}	m	n
AT3-006	3	6	1,5	3,07	-2,5	5	6,8	0,5
AT3-011	3	6,5	1,5	2,56	-2,5	5	6,7	1,5

Percolation Models for the Dilatant Permeability Concept

The percolation is known as a random geometrical distribution process that fills sites in a lattice form cluster of sites. The sites are occupied at a given time with a probability of p. If the occupation probability increases, the sites are interconnected to form structures of finite clusters. With a further increase, the occupation probability reaches a critical value p_c, which results in coupling of the clusters to form an infinite connectivity. The concept of percolation is closely associated with the permeation of fluids through fractured media.

The typical development of the acoustic emission sites during the triaxial permeability measurements is given in Fig. 7 to demonstrate the different stages in analogy to the percolation process with the initiation and growth of the connectivity in the rock salt.

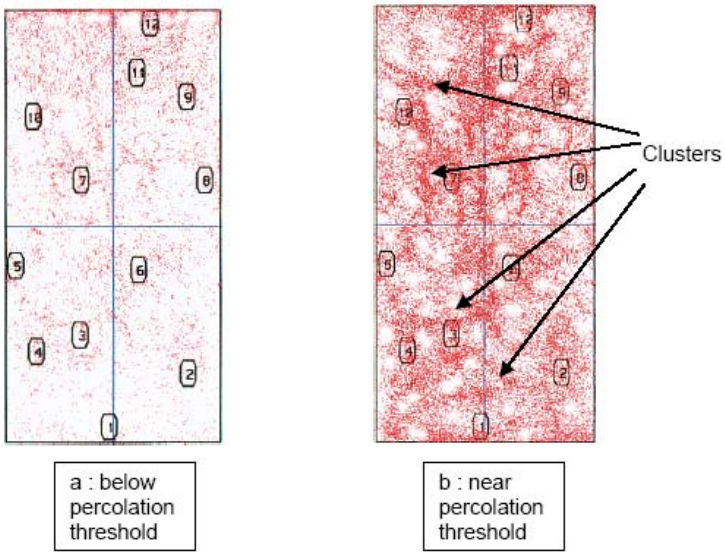

Fig. 7. Acoustic emission sites determined during the triaxial compression tests- The cross section of a cylindrical core (6x30 cm)

Fig. 7a shows that the clusters are small and isolated, the occupation probability is very low. As the deviatoric stress increases, p increases too and the clusters of opened cracks merge together and grow (Fig. 7b). This stage is considered as critical probability, i.e. $p = p_c$, where infinite clusters may exist. For an infinite cluster, there is no measuring unit a to scale the lattice properties. In other words, at p_c the lattice becomes self similar; local de-tails of the lattice become irrelevant and the lattice is said to have universal quantities which can me modeled using a fractal concept. The fractal dimension for the Asse cores before and after the triaxial measurements were determined by using the "box-counting method" as shown in Fig. 8 for the two tests.

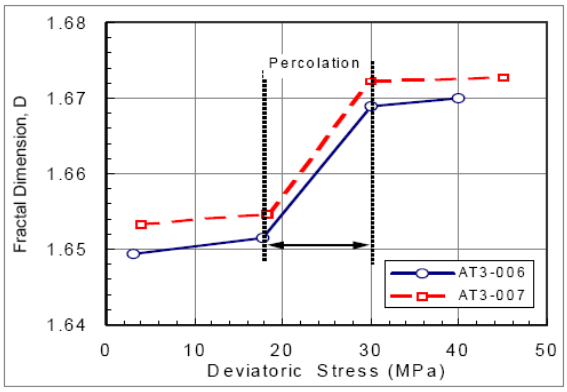

Fig. 8. Fractal dimensions of the Asse rock salt samples from microscopic measurements.

The fractal dimension above the percolation threshold probably shows the backbone clusters as an interconnected flow network. From the homogeneous distribution of this clusters it is obvious that the nature of the volume increase can be more probably related to an extension of inter-crystalline boundaries than to the development of trans-crystaline cracks.

The coincidence of the critical percolation probability and the permeability dilatancy, where the permeability begins to increase sharply, is assumed. For many physical systems near and above the percolation threshold, the physical quantities observed have power law dependencies on the system parameters. The same is valid for the permeability:

$$k \propto (p - p_c)^t \tag{9}$$

$$k = (2/15)\alpha\theta\varepsilon_v w^2 (p - p_c)^t \tag{10}$$

For a simple approach to the percolation probability above the threshold value p_c, the geometrical expression proposed by Peach, is applied. The critical percolation exponent t is introduced as the backbone cluster size in relation to the fractal dimensionality, as discussed in Yuval et al.:

$$t = B(p)D \tag{11}$$

where B(p) is the probability of the bonds belonging to the backbone. Since only a rare information is available on the stress-and time dependent functions of the geometrical parameters θ, α and ω, and the conversion of the acoustic events into a probability function is not quite clear, a dynamic modelling of the gas percolation in a permeability-dilatancy experiment was not yet possible. Therefore, the probability function was used to match the observed permeability increase in the experiment AT3-011. The geometrical parameters were derived from microscopical observations of the stressed cores in the final stage.

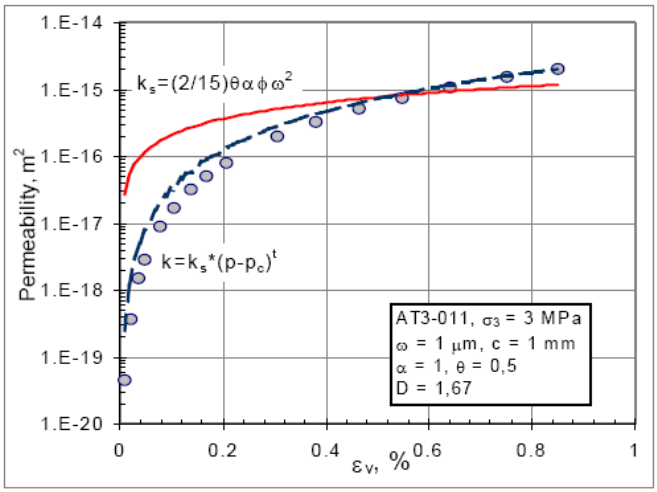

Fig. 9. Matching the results of the k-φ correlation developed for the EDZ using the simplified. Peach model and the geometric parameters from microscopic measurements.

An acceptable match was obtained for the case where t is equal to 1,3 which leads to B(p) of 0,76.

For a better definition of the dynamic percolation development below and above-near critical region, the occupation probability and percolation threshold values should be effectively coupled with measurable physical parameters. The microseismic method is a promising tool, provided that the resolution of the geometrical dimensions can be increased. For the sample size used in this study it was not yet possible.

Conclusions

The results of the experimental study of the dilatant deformation of natural samples (re-compacted) of the Asse rock salt could be used to characterize the mechanical/hydraulic behaviour of the build-up of the excavation damaged zone with the aid of semi-empirical correlations and the permeability performance is matched with a simplified percolation correlation after Peach, using measured fractal dimensions and microcrack geometry factors. The nature of the network of voids, being responsible for the observed gas conductivity, is predominantly an extension of crystal boundaries (homogeneous distribution of acoustic events) rather than prevailing transcrystalline microfractures.

***Acknowledgement**: The authors wish to thank the Federal Ministery of Research (BMBF) for funding the project and Dr. Cinar (Stanford University) and Mr. Manthei (GmUG) for their valuable contributions in the mathematical correlations and microseismic measurements and interpretation.*

References :

Bays, C. A.: Use of salt solution cavities of underground storage, Symp. On Salt, *Cleveland, Ohio 1963*.

Bieniawski, Z. T.: Mechanism of brittle fracture of rock, Part I – Theory of the fracture process, *Int. Jour. Of Rock mech. and Min. Sci., 4 (1967), 365-430*.

Borgmeier, M., Weber, J.: Permeabilitätsänderungen an homogenen modellsalzkernen, *EEK 108, 412-414, 1992*.

Carter, N. L., Horseman, S. T., Russell, J. E., Handin, J.: Rheology of rocksalt, J. of structural geology 15, *1257-1271. 1993*.

Chelidze, T., Geuguen, Y.: Evidence of fractal fracture, *Int. J. Rock mech. Min. Sci. 27 (3), 223-225, 1989*.

Chen, Y., Nishiyama, T., Kusuda, H., Kita, H. Sato, T.: Correlation between micro-crack distribution patterns and granitic rock splitting planes, *Int. J. Rock Mech. Min. Sci. 36, pp. 535-541, 1999*.

Chritescu, N., D., Hunsche, U.: Time Effects in rock mechanics, *John Wiley&Sons, 1998.*

Förster, S.: Durchlässigkeitsuntersuchungen an salzgestein, *Diss. Bergakademie Freiberg, 1971*.

Gertsch, L. S.: Three dimensional fracture network models from laboratory-scale rock samples. *Int. J. Rock Mech. Min. Sci. Geomech. Abstr., 32 (1), 85-91. 1995*.

Häfner, F., Belohlawek, U., Behr, A., Förster, S., Pohl.: In-situ ermittlung von strömungskennwerten natürlicher salzgesteine in ALZ gegenüber gas und salzlösungen unter den gegebenen spannungsbedingungen im gebirge, *BMBF 02 C05276, 1999*.

Haimson, B., Chang, C.: A new true triaxial cell for testing mechanical properties of rock, and its use to determine rock strength and deformability of westerly granite, *Int. J. Rock Mech. Min. Sci. 37, p. 285-296., 2000*.

Hamami M.: Simultaneous effect of lading rate and confining pressure on the deviator evolution in rock salt, *Int. Jour. Of Rock mech. And Min. Sci., 36 (1999), 827-831*.

Handin, J., Hager, R. V., Friedmann, M., Feather, J. N.: Experimental deformation of sedimentary rocks under confining pressure pore pressure tests, *Bull. Am. Assoc. Pet. Geol., V 47, May 1963, 717-755*.

Hou, Z., Düsterloh, U., Lux, K.-H.: Neue aspekte zum tragverhalten von salzkavernen und zu ihrem geotechnischen sicherheitsnachweis, *Teil 1 und 2 in Erdöl Erdgas Kohle(115) 1999, 122-127, 196-206*.

Hunsche, U., Hampel, A.: Rock salt – the mechanical properties of the host rock material for a radioactive waste repository, *Engineering Geology 52, p. 271-291. 1999*.

Hunsche, U.: Dermination of dilatancy boundary and damage up to failure for four types of rock salt at different stress geometries, *Fourth conference on the mechanical behaviour of salt, Proceedings, 163-173*.

Hunsche, U.: Determination of the dilatancy boundary and damage up to failure for four types of rock salt at different stress geometries, *In: Aubertin, M., Hardy Jr., H.R. (Eds.), The mechanical behaviour of salt IV; Proc. Of the fourth conf., Montreal 1996. Trans Tech. Publications, Clausthal, pp. 163-174, 1998*.

Li, H. B., Zhao J., Li., T. J.: Triaxial compression tests on a granite at different strain rates and confining pressures, *Int. Jour. Of Rock mech. And Min. Sci., 36 (1999), 1057-1063* .

Nolte, D. D., Pyrak-Nolte, L. J., Cook, N.G.W.: The fractal geometry of flow paths in natural fractures in rock and the approach to percolation, *PAGEOPH, Vol. 131, Nos 1/2. 1989*.

Peach C., J.: Influence of deformation on the fluid transport properties of salt rocks, *PhD Thesis, Utrecht, 1991*.

Peach, C. J.:. Influence of deformation on the fluid transport properties of salt rocks. PhD Dissertation, Utrecht: Instituut voor Aardwetenschappen der Rijksuniversiteit Utrecht, Holland,1990.

Pusch, G., Weber, J. R.: Correlation of rock permeability and anisotropic stress conditions for the integration of rock mechanical and hydraulic flow models, *SCA 9826, den Hague, 14-15 Sept. 1998*.

Ropp, T., Kern, H., Schulze, O.: Evolution of dilatancy and permeability in rock salt during hydrostatic compaction and triaxial deformation, *Jour. Of Geoph. Res., 106, 2001, 4061-4078*.

Sambeek, L. L., Ratigan, J. L., Hansen, F .D.: Dilatancy of rock salt in laboratory tests, Int. Jour. *Of Rock mech. and Min. Sci., 30 (1993), 735-739*.

Schulze, O., Popp, T., Kern, Hartmut, K.: Development of damage and permeability in deforming rock salt, *Engineering Geology, 61, 2001, 163-180*.

Serata, S., Fuenkajorn, K.: Formulation of a constitutive equation for salt, *7th Symp., on Salt., 483-488, 1993*.

Spiers, C .J., Carter, N. L.: Microphysics of rocksalt flow in nature, Fourth conference on the mech. behaviour of salt, *The Penn State University, June 17-18. 1996*.

Spiers, C. J., Peach, C. J., Brzesowsky, R. H., Schutjens, P. M. T. M., Liezenberg, J. L., Zwart, H.J.: Long-term rheological and transport properties of dry and wet salt rocks, Nuclear Science and Technology, *EUR 11848 EN, Office for Official Publications of the European Communities, Luxembourg. 1989.*

Spiers, C. J., Shutjens, P. M. T. M., Brzesowsky, R. H., Peach, C. J., Liezenberg, J. L., Zwart, H.J.: Experimental determination of constitutive parameters governing creep of rocksalt by pressure solution, in: *Deformation Mechanics, Rheology and Tectonics (edited by Knipe, R.J. and Rutter, E.H.), Spec. Publs. Geol. Soc. Lond., 54, 215-227. 1990*.

Spiers, C. J., Urai, J.,. Gordon, S. L: The effect of brine (Inherent or added) on rheology and deformation mechanisms in salt rock, Second conference on the mech. behaviour of salt, *Federal Institute for Geosciences and Natural Resources, Hanover, Germany, September 24-28. 1984*.

Stormont, J. C.: Gas permeability changes in rock salt during deformation, *Dissertation, 1990*.

Urai, J. L., Spiers, C. J., Peach, C. J., Franssen, R. C. M. W., Liezenberg, J. L.: Deformation mechanics operating in naturally deformed halite rocks as deduced from micro-structural investigations, *Geol. En Mijnb., 66, 164-176. 1987*.

Urai, J. L., Spiers, C. J., Zwart, H. J., Lister, G. S.: Weakening of rocksalt by water during long-term creep, *Nature 324, 554-557. 1986*.

Weber, J. R.: Untersuchung zur Permeabilitätsdilatanz kristalliner gesteine unter deviatorischer belastung, *Dissertation, TU Clausthal 1994*.

Weidinger, P., Blum. W., Hunsche, U., Hampel, A.: The influence of friction on plastic deformation in compression tests, *Phys. Stat. Sol., 156, 1996*.

Yuval g., Aharogny, A., Mandelbrot, B., Kirckpatrick, S.: Solvable fractal family, and its possible relation to the backbone at percolation, *Physical Review letters, V. 47, 25, 1981, 1771-1774*.

Zhang, Z. X., Kou, S. Q., Jiang, L. G., Lindqvist, P. A: Effects of loading rate on rock fracture: Fracture characteristics and energy partionning, Int. *Jour. Of Rock mech. And Min. Sci., 37 (2000), 745-762*.

Zhang, Z. X., Kou, S. Q., Yu J., Yu, Y., Jiang L. G., Lindqvist P. A.: Effect of loading rate on rock fracture, Int. *Jour. Of Rock mech. And Min. Sci., 36 (1999), 567-611*

Zhang, Z. X., Kou, S. Q., Jiang, L. G., Lindqvist, P. A.: Effects of loading rate on rock fracture: Fracture characteristics and energy partitioning, Int. *J. Rock Mech. Min. Sci. 37, pp. 745-762, 2000*.